DNA Bubble Formation in Transcription Initiation†

Vladimir Tchernaenko,‡ Herbert R. Halvorson,‡ Mikhail Kashlev,§ and Leonard C. Lutter*,‡

Molecular Biology Section, Bone and Joint Center, Henry Ford Hospital, Detroit, Michigan 48202, and Molecular Mechanisms of Transcription Section, NCI Center for Cancer Research, Frederick Cancer Research and Development Center, Frederick, Maryland 27102

Received June 29, 2007; Revised Manuscript Received November 15, 2007

ABSTRACT: The properties of the DNA bubble in the transcription open complex have been characterized by topological analysis of DNA circles containing the *lac* UV5 promoter or the PR promoter from bacteriophage lambda. Topological analysis is particularly well suited to this purpose since it quantifies the changes in DNA duplex geometry caused by bubble formation as well as by superhelical DNA wrapping. The duplex unwinding that results from bubble formation is detected as a reduction in topological linking number of the DNA circle, and the precision of this measurement has been enhanced in the current study through the use of 8 or 10 promoter copies per circle. Several lines of evidence indicate that the linking number change induced by open complex formation is essentially all due to bubble generation, with very little derived from superhelical wrapping. Accordingly, the linking number change of −1.17 measured for the *lac* UV5 promoter indicates that the size of the *lac* UV5 bubble is about 12.3 base pairs, while the change of −0.98 measured for the lambda PR promoter indicates that the lambda PR bubble is 10.3 base pairs. It was also found that the presence or absence of magnesium ion had little effect on the value of the linking number change, a result that resolves the uncertainty associated with use of chemical probes to study the effect of magnesium on bubble size. Finally, the magnitude of linking number change increases progressively when the 3′ end of a transcript is extended to +2 and +3 in an abortive initiation complex. This indicates that the transcription bubble expands at its leading edge in the abortive complex, results that confirm and extend the proposal of a DNA "scrunching" mechanism at the onset of transcription. These results are relevant to several models for the structure of DNA in the functional open complex in solution, and provide an important complement to the structural information available from recent crystal structures.

Transcription initiation is a process that occurs via multiple steps as illustrated by the minimal scheme

$$R + P \leftrightarrow RPc \leftrightarrow RPi \leftrightarrow RPo$$

The process begins with RNA polymerase (R) binding to a promoter (P) to form a "closed" complex (RPc, also termed I_1), after which it converts to an intermediate complex (RPi, also termed I_2) and finally to an open complex (RPo) [reviewed in (*1*, *2*)]. The open complex is the active complex for initiation of transcription, and its formation is accompanied by the denaturation of a discrete section of promoter to form a transcription "bubble". The various intermediates in the process have been characterized in solution by kinetic analysis as well as by structural approaches such as chemical and enzymatic footprinting. The most detailed structural information for several of these complexes has come from the impressive progress made in the characterization of the crystal structures of RNA polymerase alone and in the elongation complex containing template and short nascent RNA [reviewed recently (*3*)], although a crystal structure of the open promoter complex has yet to be described. However, while the crystal structures of elongation complexes reveal unprecedented detail, the extent to which they represent the structures of active complexes in solution remains unknown, and they as yet do not provide a full description of the complex DNA (*4*, *5*). For example, the cocrystals to date contain a length of DNA that is considerably less than that which footprinting studies indicate is associated with the polymerase in the open complex in solution. Furthermore, none of the crystal structures contain a complete transcription bubble. Finally, none of the crystallography data provides information of the dynamics of the bubble structure exhibited in solution.

This issue has been addressed by numerous complementary methods that have been used to characterize the solution structures of complete transcription complexes. One such solution method that has been widely used to analyze the intact transcription bubble is chemical probe analysis. Thus direct evidence for the opening of 10−14 bp of promoter DNA during open complex formation comes from the use of chemical reagents that react more readily with single stranded DNA than with duplex DNA (*6*−*11*). These studies find that open complex formation causes enhanced reactivity to agents such as dimethyl sulfate and $KMnO_4$ in the region between −12 and +2 at several promoters. In addition, the

† This work was supported in part by grants from the National Institutes of Health (GM49988 and GM56216).

* Corresponding author. E-mail: llutter1@hfhs.org. Tel: 313-916-8681. Fax: 313-916-8064.

‡ Henry Ford Hospital.

§ Frederick Cancer Research and Development Center.

10.1021/bi701289g CCC: $40.75
Published on Web 01/19/2008

region of reactivity in the absence of magnesium was observed to be about 8−10 bp and not encompass the start site, while in the presence of magnesium the reactivity expanded to at least 15 bp and encompassed the start site (*10*−*12*). It was concluded that there are two forms of open complex, with the one in the presence of magnesium competent for transcription initiation.

However, while the chemical probe approach has proven very useful in determining the location and estimating the size of the bubble, there are a number of uncertainties associated with the interpretation of the results: (1) Although the chemical probes used do react preferentially with denatured DNA, other distortions of the duplex can also result in reactivity. Thus the method is not strictly specific for a transcription bubble (*11*, *13*, *14*). (2) The reacted bases represent only a small fraction [e.g., <5% (*15*)] of the complexes, raising an uncertainty about whether this small fraction is representative of the total population of complexes [this common problem is discussed in (*16*)]. (3) The reagents used can react with residues on the polymerase, leading to its inactivation (*13*, *17*). This raises a question about whether the results represent the active complex or an inactive, and perhaps distorted, complex (*17*, *18*). (4) Portions of polymerase can protect nucleotides that are part of the bubble from reaction with the probe (*19*−*22*), leading to incorrect conclusions about the size, existence, or location of the bubble. (5) Incomplete sampling of the sequence due to the base specificity of many reagents makes a precise determination of bubble size difficult. (6) Different reagents can give different results on the same promoter, leading to opposite conclusions about the presence of a bubble (*23*). (7) If the bubble is dynamic, i.e., "breathes", then reactivity will tend to represent the most open extent of the breathing. This leads to an overestimate of the average bubble size. (8) Factors such as Mg^{2+} can increase reactivity of negatively charged chemical probes such as permanganate ion by reducing ionic repulsion of the negative phosphate groups of DNA (*2*, *10*, *24*−*26*). This can lead to the incorrect conclusion that Mg^{2+} causes an increase in the bubble size. (9) If the nucleotide bases in the single stranded DNA are involved in stacking interaction, it may affect their reactivity to the chemical probes.

These limitations of the use of chemical probe analysis can be addressed through the use of other, complementary methods for structural characterization of the open complex bubble in solution. DNA topological analysis is one such method that has been used to provide an independent assessment of bubble size. It is a "noninvasive" method: it characterizes the structure of an active transcription complex in solution without perturbation or inactivation of the complex. It measures the polymerase-induced change in the topological linking number, which is the number of times one strand of the double helix crosses over the other in covalently closed circular DNA [reviewed in (*27*−*30*)]. For example, if open complex formation induces a bubble of 10.5 bases, this will cause an unwinding of one turn of DNA duplex, i.e., a loss of one strand crossing. If the complex is formed on a promoter in circular DNA which is then treated with topoisomerase, the linking number of the complex DNA will be reduced by one relative to that of similarly treated bare DNA. In addition, wrapping of the DNA in a superhelical path (chiral wrapping) will also cause a linking number change, e.g., a single left-handed superhelical turn also induces a linking number change of −1.0. The linking number difference is readily quantified by electrophoresis of the two DNA samples in an agarose gel.

Early topological studies of polymerase complexes did not analyze specific known prokaryotic promoters, leading to an uncertainty about polymerase occupancy due to the inability to demonstrate promoter saturation by titration analysis (*31*−*34*). Such saturation was demonstrated in an analysis of open complex formation at the *lac* UV5 promoter, where Amouyal and Buc (*35*) concluded that complex formation induced a linking number change of −1.7. Chemical probe results (*7*, *8*, *21*, *22*) predicted that bubble formation would induce a change of only ∼−1. Following from the nucleosome example in which the linking number change contains contributions from both duplex winding change and superhelical wrapping (*36*), Amouyal and Buc proposed that the excess −0.7 linking number change represents a left-handed superhelical wrap of about 0.7 turn (*35*). This has been widely cited as some of the earliest evidence for wrapping of DNA on the polymerase surface [reviewed in (*37*)].

There are some difficulties with this interpretation of these results. First, the presence of several additional promoters in the plasmids meant that the *lac* UV5 contribution was only a minor portion of the total polymerase-induced linking number change, i.e., there was a substantial "background" due to additional promoters. This, coupled with the use of only a single copy of the *lac* UV5 promoter, limited the precision of the measurement. Second, similar studies of other promoters (*38*, *39*) obtained smaller changes that were closer to the −1 predicted by the chemical probe studies, i.e., values that do not represent an excess of −0.7 linking number difference that leads to invoking superhelical DNA wrapping on the polymerase surface.

To address these various issues, we have developed a modified topological characterization of the transcription complex. The analysis is performed on DNA circles that contain multiple copies (8 or 10) of a single promoter only, resulting in an amplified linking number change signal. This amplification of the linking number change as well as the absence of other promoters means that the linking number change per promoter can be measured with high precision and specificity. Both the *lac* UV5 promoter and bacteriophage lambda PR promoter (λP_R[1]) have been analyzed. Several types of experimental results indicate that the linking number change represents bubble formation and not superhelical wrapping of DNA around the open complex. Accordingly, the value −1.17 measured for the *lac* UV5 complex indicates a bubble of 12.3 bases, while the value of −0.98 measured for λP_R indicates a bubble of 10.3 bp. In addition, analysis of λP_R abortive initiation complexes containing RNA transcripts extending to positions +2 and +3 indicates that the bubble expands with increasing transcript length. Finally, it was found that the bubble size was essentially the same in the presence or absence of Mg^{2+}, a finding that contrasts with the conclusions of chemical probe studies (*10*, *11*). The relevance of these results to structures of intermediates in the process of transcription initiation as well as the use of

[1] Abbreviations: λP_R, the bacteriophage lambda PR promoter; ΔL, DNA topological linking number change; bp, base pair.

chemical probes in bubble characterization is discussed. The accompanying paper (*40*) describes a companion study analyzing DNA bending in the open complex and the +3 abortive initiation complex.

MATERIALS AND METHODS

Plasmid Construction. Plasmid pLU875, a plasmid containing 8 copies of the *lac* UV5 promoter, was generated as follows. A PCR reaction employing appropriate primers with plasmid pRLG593 [(*41*), kindly provided by Dr. R. Landick] as template was used to generate a fragment containing the *lac* UV5 promoter (−59 to +100 from pRLG593) with *Sph*I and *Ava*I sites on the upstream end of the fragment and a *Sal*I site on the downstream end. This was cleaved with *Sph*I and *Sal*I and cloned into pBR322 that was digested with *Sph*I and *Sal*I using Stbl4 (Invitrogen) as the host. The initiator fragment procedure (*42*) was used to oligomerize the 875 bp *Ava*I fragment to generate pLU875, a construct that contains 8 copies of the fragment. To generate the circle cLU875 (see Figure 1) containing only those 8 repeats and no vector promoters, pLU875 was digested with *Nsp*I, after which the fragment containing the 8 *lac* UV5 promoters was purified and ligated to form a 7396 bp circle. For some experiments a single nick was introduced into cLU875 by incubation with *Nb.Bpu*10I (New England Biolabs). The pNPR*nnn* plasmids and the circularized cNPR*nnn* fragments were constructed as described (*40*). They comprise a "rotational variant" set that is used to measure the bend angle of λP_R initiation complexes, but they are also used here to analyze the transcription bubble. The "*nnn*" refers to the length of a fragment containing the λP_R that is present in multiple copies in the construct, i.e., "*nnn*" is the repeat length. For example, pNPR149 contains 5 tandem repeats of a 149 bp fragment containing the λP_R promoter [constructed using the initiator fragment procedure (*42*)]. The *Pst*I/*Apo*I fragment containing the 5 repeats was self-ligated to form cNPR149, a 2888 bp head-to-head dimer circle that contains 10 copies of the λP_R promoter (see Figure 1). Only a very minor fraction of the total linking number change derives from the repeat-length-variable contribution [termed ΔL_{SH} and due to the contribution arising from the presence of a bend, discussed in detail in (*40*)], so constructs with different repeat lengths were used interchangeably in this bubble study. Note also that the head-to-head arrangement of the two blocks of 5 repeats does not affect the topological measurements since the contribution of duplex unwinding to linking number change is unaffected by the relative orientation of the two blocks of 5 promoters.

Open Complex Formation and Analysis. For the titration in Figure 1, the binding reaction involved incubating the indicated amounts of histidine-tagged RNA polymerase holoenzyme (*43*) with *Nb.Bpu*10I-nicked cLU875 (0.11 nM, 0.88 nM *lac* UV5) in K-Hepes (pH 8), 137 mM KCl, 0.2 mM EDTA, 0.045 mM NAD (Sigma), 9% glycerol, 0.1 mg/mL acetylated BSA (NEB), and 10 mM $MgCl_2$ for 5 min at 37 °C. Then *Escherichia coli* DNA ligase (182 units/mL; New England Biolabs) was added, followed by a further 5 min incubation at 37 °C. Samples were then extracted with phenol and ethanol precipitated, after which they were fractionated by two-dimensional electrophoresis in an agarose gel. The first dimension (top to bottom in the figures) was in TBE buffer (89 mM Tris-borate, 2 mM EDTA, pH 8.2) plus 0.33 μg/mL chloroquine diphosphate. Topoisomers are positively supercoiled in the first dimension in all figures, meaning linking number decreases with decreasing mobility. A short second dimension was then run (left to right) in TBE plus 0.1 μg/mL ethidium bromide to separate the topoisomers from the nicked and linear species on the diagonal. The gel was stained with ethidium bromide and scanned (FMBio), after which the density profile of each topoisomer distribution was obtained (MultiAnalyst, BioRad) and its center determined [see (*44*) for details]. Measurement of linking number difference (ΔL) has been described previously [e.g. (*45*−*48*), reviewed in (*49*)]. Briefly, the polymerase-induced linking number difference is the difference between the mean linking number of the polymerase−bound circle following ligation (L_{+RP}) and that of the circle ligated in the absence of polymerase (L_{-RP}), i.e., $\Delta L = L_{+RP} - L_{-RP}$. Thermal energy present in solution at the time of ligation results in the generation of a distribution of topoisomers whose envelope is Gaussian, and the mean linking number of the sample is the center of that distribution. Examples of densitometer traces of distributions for polymerase-bound and bare samples are shown at the bottom of Figure 1, with the distribution center indicated by an arrowhead. It should be noted that while the linking number of a single DNA molecule is necessarily an integer, the mean linking number is not limited to integer values since it is the center of a distribution of integer values. Consequently the linking number difference is also not limited to integer values.

The temperature analysis in Figure 2 was performed as follows: open complexes were formed on relaxed closed circular cLU875 or cNPR153 with a saturating level (10-fold or greater molar excess over promoter sites) of histidine-tagged RNA polymerase holoenzyme as described above but using an incubation of 15 min at 37 °C. Samples were then removed and incubated with wheat germ topoisomerase I (100 units/mL; Promega) at the indicated temperatures for 30 and 120 min (two time points were used to be certain the relaxation was complete). Wheat germ topoisomerase I was used in this experiment (rather than ligation as used above) because of its demonstrated ability to relax DNA to completion even at 0 °C (*45*), although this also required beginning with covalently closed DNA (the linking number change at 37° was the same for the two methods). The extracted DNAs were then fractionated by one-dimensional electrophoresis in agarose gels that included the indicated concentrations of chloroquine diphosphate to achieve optimal separation of topoisomers. For any of the cNPR*nnn* (in contrast to cLU875), the extended range of supercoil densities resulting from the small size of the circle coupled with the 10 promoter copies required a connector series (*40*, *48*) to relate the linking number registers of the two gels shown in Figure 2A. The value of the linking number of bare DNA at each temperature was obtained from a linear regression analysis of a plot of linking number versus temperature (Figure 2C), and this was subtracted from the value obtained for the sample incubated with polymerase at each respective temperature to obtain the linking number change. This was plotted versus temperature (Figure 2D). Fitted to the data was a version of the van't Hoff equation: $\Delta L/\Delta L_{RPo} = 1/(\exp((\Delta H/R)((1/T) - (1/T_m))))$, where ΔL is the linking number change at the given temperature T (K), ΔL_{RPo} is the linking number change of the open complex, R is the gas

constant (1.987 cal deg^{-1} mol^{-1}) and the enthalpy (ΔH) and melting temperature (T_m) are parameters.

The rate of decay of the linking number change (Figure 3A,B) after a 37 °C to 12 °C shift was determined as follows: open complexes were formed on *Nb.Bpu*10I-nicked cLU875 at 37° as described above. The temperature was then reduced to 12 °C, and samples were removed at the designated times, followed by the addition of *E. coli* ligase (450 units/mL) and a further incubation of 1 min. Each sample was then extracted with phenol and ethanol precipitated, after which the samples were fractionated by two-dimensional electrophoresis as described for Figure 1 above. A single-exponential decay function was fitted to the data. Nick ligation is more convenient to use than topoisomerase relaxation for kinetic experiments because it eliminates any concern about incomplete relaxation.

The demonstration in Figure 3D of post-shift occupancy using restriction digestion protection (*50*−*52*) was performed with the 332 bp *Nci*I/*Psh*AI fragment (containing the *lac* UV5 promoter) purified from pLU875. Open complexes were formed on this fragment at 37 °C as described above, after which half the sample was shifted to 12 °C for 2 min. *Hpa*II was then added to each sample, and the incubation was continued for an additional 2 min. Samples were then extracted with phenol, precipitated with ethanol, and fractionated by electrophoresis in a 7% acrylamide gel.

Demonstration of post-shift occupancy by bandshift analysis (*53*, *54*) was performed using the same *Nci*I/*Psh*AI fragment. Open complexes were formed at 37 °C, after which the temperature was dropped to 12 °C and the incubation continued for 2 min. The sample was immediately loaded onto a 0.7% agarose gel in 0.5 × TBE equilibrated at 12 °C followed by electrophoresis for 9 min at 250 V per 10 cm. An in-gel thermocouple indicated that the gel temperature remained at 12 ± 1 °C during the electrophoresis. The gel was then stained with ethidium bromide and imaged as described above.

Analysis of Abortive Initiation Complexes. Abortive initiation complexes (Figure 4A) were analyzed as follows: the indicated oligoribonucleotide (0.066 mM, Dharmacon) was added to open complexes preformed on the indicated cNPR*nnn* (26 nM, 260 nM RNA polymerase), and the sample was incubated for 10 min at 37 °C [analysis using of radioactively labeled GCAUG and size exclusion chromatography confirmed its stable binding to the λP_R open complex (not shown)]. Then *E. coli* DNA ligase (182 units/mL; Invitrogen) was added, followed by a further 5 min incubation at 37 °C. Samples were then extracted with phenol and ethanol precipitated, after which they were fractionated by either one-dimensional electrophoresis (0.02 μg/mL ethidium bromide in TBE) or two-dimensional electrophoresis in an agarose gel as described above.

The effect of Mg^{2+} on the open complex ΔL (Figure 4) was determined as follows: open complexes were formed using the indicated amounts of histidine-tagged RNA polymerase holoenzyme added to relaxed cNPR149 in K-Hepes (pH 7.5), 150 mM NaCl, 40 mM KCl, 0.1 mM EDTA, 10% glycerol, 0.1 mg/mL acetylated BSA, with and without and 10 mM $MgCl_2$. Samples were incubated 10 min at 37 °C, after which wheat germ topoisomerase I (200 units/mL) was added and the incubation was continued for 60 min at 37 °C. Wheat germ topoisomerase I was used in this experiment because, unlike DNA ligase, it is active in the presence or absence of Mg^{2+}. Samples were extracted with phenol, ethanol precipitated, and fractionated by two-dimensional electrophoresis in which the TBE buffer of the first dimension contained 0.022 μg/mL ethidium bromide and that of the second dimension contained 0.1 μg/mL ethidium bromide.

RESULTS

Open Complex Formation on a Circle Containing a Single Promoter in Multiple Copies. Previous studies that measured the linking number change induced by initiation complex formation suffer from limited precision due to analysis of only one promoter copy (*35*, *38*, *39*) as well as the presence of other promoters in the circle (*35*, *39*). To address these concerns, measurement precision was enhanced by amplifying the linking number change signal through the introduction of multiple, tandemly repeated copies of the promoter to be analyzed. Thus to study open complex formation at the *lac* UV5 promoter, the plasmid pLU875, containing 8 tandemly repeated *lac* UV5 promoters, was constructed using the initiator fragment strategy (*42*) (see Materials and Methods). To eliminate the complication of the presence of the additional promoters present in the cloning vector, a fragment containing only the 8 *lac* UV5 repeats was generated by *Nsp*I digestion, after which the purified fragment was circularized by ligation to form cLU875 (Figure 1, top left). To study the λP_R promoter, similar methods were used to generate a family of circles, generally termed cNPR*nnn* (Figure 1, top right), containing 10 copies of the λP_R promoter, arranged as two blocks of 5 promoters in a head to head orientation (*40*). This family was constructed for measuring the DNA bend angle of initiation complexes using rotational variant analysis (*40*) and is composed of constructs in which the repeat length (*nnn*) varies from 143 bp (cNPR143) to 157 bp (cNPR157).

The bottom panel of Figure 1 shows a titration curve in which increasing amounts of *E. coli* RNA polymerase holoenzyme were added to singly nicked cLU875 to form open complexes, after which the nick was ligated (see Materials and Methods). DNA samples were fractionated by electrophoresis in an agarose gel to resolve topoisomers, and images of gels from two experiments encompassing different ranges of RNA polymerase concentration are shown at the center of Figure 1. Samples incubated in the absence of RNA polymerase (lanes a, e) show topoisomer distributions that are well down the gel. These topoisomers are positively supercoiled under the gel conditions used, with the linking number decreasing with decreasing mobility. Addition of increasing amounts of RNA polymerase in the incubation to form open complexes causes the respective topoisomer distributions to move progressively up the gel (lanes b−d, f−k), indicating that open complex formation causes a reduction in the linking number. Moreover, the mobilities of the distribution centers are virtually equivalent over the 13-fold range of higher polymerase concentrations (lanes f−k), demonstrating that the 8 promoter sites are saturated and that there is minimal nonspecific binding. The mean linking number change (ΔL) is the difference in linking number units between the center of the topoisomer distribution of the open complex and that of the bare DNA. This difference was $\Delta L = -9.4 \pm 0.1$ (average ± SD for

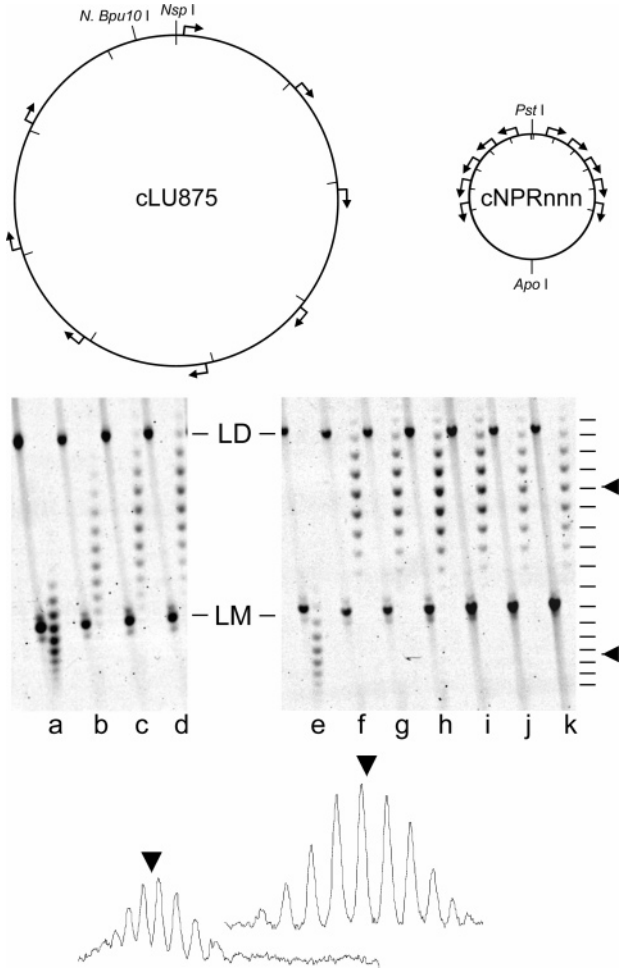

FIGURE 1: DNA circles and open complex titration. At the top left is the structure of cLU875, a circle containing 8 tandem repeats of an 875 bp *Ava*I fragment that contains the *lac* UV5 promoter (arrows). The *Ava*I sites are marked inside the circle. At the top right is the structure of cNPR*nnn*, a circle containing 10 copies of the λP_R promoter arranged in two blocks of 5 tandem repeats (*40*). Below this are shown the results of titration experiments in which samples of nicked cLU875 (0.11 nM, 0.88 nM *lac* UV5) were incubated with increasing amounts of RNA polymerase to form open complexes, after which each sample was incubated with *E. coli* DNA ligase to covalently close the circle. Purified DNAs were then fractionated by two-dimensional electrophoresis in an agarose gel. The first dimension (top to bottom) contained 0.33 μg/mL chloroquine diphosphate to resolve the topoisomers as positively supercoiled species, so the linking number decreases with decreasing mobility (this is the case with all gels in subsequent figures as well). A short second dimension (left to right) in 0.07 μg/mL ethidium bromide was used to separate the topoisomers from nicked and linear species that remain on the diagonal. The two gels shown represent two separate titrations using different ranges of polymerase concentrations. The image of the ethidium-stained gel is shown. The concentration of RNA polymerase (nM) was (a) 0; (b) 5; (c) 10; (d) 15; (e) 0; (f) 30; (g) 60; (h) 100; (i) 200; (j) 300; (k) 400. The mobilities of the linear monomer (LM) and linear dimer (LD) are indicated; the linear dimer is ligation product of two *Nsp*I monomer fragments. The dashes at the right indicate the mobilities of the topoisomers in the right gel. The upper arrowhead at the right of the left gel indicates the center of the topoisomer distributions of polymerase-bound samples f−k, while the lower arrowhead indicates that of the sample ligated as bare DNA (lane e). At the bottom are scans of lane e (left scan, top of gel on left) and lane i (right scan), with the center of each distribution (corresponding to the mean linking number, see Materials and Methods) marked with an arrowhead. The RPo linking number difference (ΔL) is the difference in topoisomer bands (small peaks) between the two arrowheads, i.e., −9.4 for this pair of samples.

hyperbolic fit of 7 points), which is -1.17 ± 0.01/open complex. This value contrasts with a previous measurement, discussed in the introduction, of −1.7/open complex (*35*). That measurement was interpreted as evidence for DNA wrapping on the open complex because it was about −0.7 more than would be expected from bubble formation. In contrast, bubble formation provides a sufficient explanation for our measurement: the −1.17 measured in Figure 1 corresponds to a bubble of about 12 bp (at 10.5 bp/duplex turn). This is in fact about the size of the bubble predicted from chemical probe experiments (10−14 bp, see above), indicating that the linking number change directly represents bubble formation with little contribution from superhelical DNA wrapping (see Discussion).

Temperature Dependence of the Linking Number Change. A temperature analysis was performed to further establish the direct relationship between linking number change and bubble formation implied by the results above. Chemical probe experiments indicate that when an open complex is formed at 37 °C followed by dropping the temperature to progressively lower values for probing, the bubble undergoes an abrupt collapse with a midpoint (T_m) of about 20 °C for *lac* UV5 (*21*, *22*). Figure 2 shows the results of a topological version of that experiment. Open complexes were formed on relaxed, non-nicked circles at 37 °C, after which samples were shifted to a series of lower temperatures. Each sample was then relaxed with topoisomerase [topoisomerase relaxation of covalently closed DNA was used here in place of ligation closure because it had been previously demonstrated that wheat germ topoisomerase I remains active down to 0 °C (*45*)], followed by analysis of the extracted DNAs by agarose gel electrophoresis. This analysis was performed on cLU875 (Figure 2B) as well as cNPR153 (Figure 2A). It can be seen in the left panel of Figure 2A that the topoisomer distributions move down the gel with decreasing relaxation temperature, demonstrating that the linking number of the circle containing 10 λP_R open complexes increases as the temperature is lowered. However, at least part of this increase is due to the fact that the DNA duplex of the entire circle winds up as the temperature is lowered (*55*, *56*). This contribution was quantified by performing a parallel analysis on bare DNA, the results of which are shown in the right panel. The bare DNA results for cNPR149 from Figure 2A as well as those for cLU875 from Figure 2B are plotted in Figure 2C. Here it can be seen that both constructs generate straight lines, as expected, with temperature coefficients that agree with previous studies (*55*, *56*).

The results of the regression analyses in Figure 2C were used to provide precise values for bare DNA. These were then subtracted from the respective values obtained from the open complex samples to give the linking number change at each temperature. The results for the two promoters are plotted in Figure 2D. The data for the *lac* UV5 construct (filled symbols) show that the linking number difference is lost as a single abrupt transition as the temperature is lowered. A van't Hoff equation fit yields values for T_m of 19.8 ± 0.5 °C. This value is comparable to that obtained from chemical probe studies (*21*, *22*) and thus indicates that the linking number change of the open complex represents bubble formation. Further support for this proposal is provided by the results of a similar analysis of the λP_R promoter shown in Figure 2D: the midpoint (T_m) of the

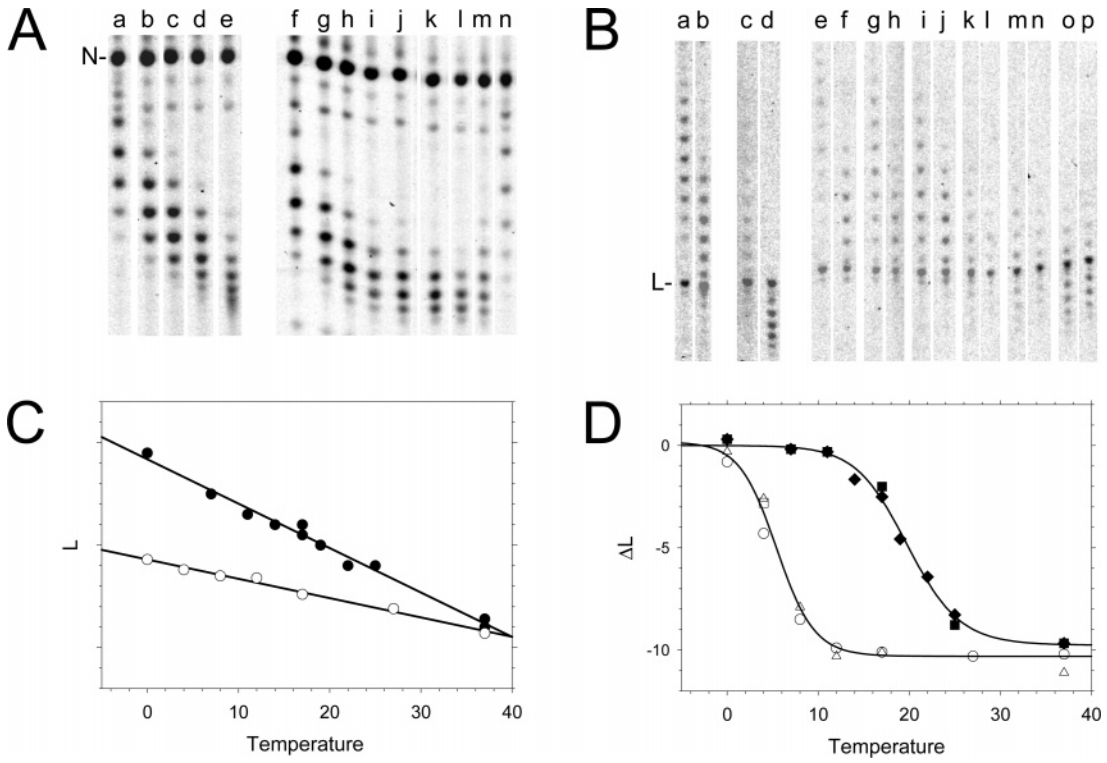

FIGURE 2: The linking number change following a shift down from 37 °C. (A) Temperature dependence of the λP_R linking number change. Open complexes were formed on cNPR153 by incubation with RNA polymerase at 37 °C, after which samples were transferred to the indicated temperatures and incubated with topoisomerase I (see Materials and Methods). The purified DNAs of the samples were fractionated by one-dimensional electrophoresis in agarose gels under the appropriate conditions to resolve closed circular DNAs as positively supercoiled topoisomers. The ethidium stained images of the gels are shown. On the left is shown an agarose gel that was run in the presence of 3.0 μg/mL chloroquine diphosphate with polymerase-bound samples relaxed at (a) 37 °C; (b) 27 °C; (c) 17 °C; (d) 12 °C; (e) 8 °C. On the right is shown an agarose gel that was run in the presence of 0.3 μg/mL chloroquine diphosphate with samples of bare DNA relaxed at (f) 37 °C; (g) 27 °C; (h) 17 °C; (i) 12 °C; (j) 8 °C; (k) 4 °C; (l) 0 °C. Also run on this gel were polymerase-bound samples relaxed at (m) 4 °C; (n) 0 °C. The mobility of the nicked species (**N**) is indicated. (B) Temperature dependence of the *lac* UV5 linking number change. A similar analysis was performed on cLU875. Shown is an agarose gel that was run in the presence of 0.6 μg/mL chloroquine diphosphate on which was run polymerase-bound samples relaxed at (a) 37 °C; (b) 25 °C. A second gel run in the presence of 0.5 μg/mL chloroquine diphosphate contained samples relaxed at 22 °C that were (c) polymerase-bound; (d) bare DNA. A third gel run in the presence of 0.3 μg/mL chloroquine diphosphate containing samples that were relaxed at (e) 19 °C, polymerase-bound; (f) 19 °C, bare; (g) 17 °C, polymerase-bound; (h) 17 °C, bare; (i) 11 °C, polymerase-bound; (j) 11 °C, bare; (k) 7 °C, polymerase-bound; (l) 7 °C, bare; (m) 4 °C, polymerase-bound; (n) 4 °C, bare; (o) 0 °C, polymerase-bound; (p) 0 °C, bare. The mobility of the linear (**L**) fragment is indicated. (C) Temperature dependence of the linking number of the bare DNAs. The temperature dependence of the linking number (**L**) of the bare cNPR153 DNA (results from the left gel in part A above) is plotted as open circles, while that of cLU857 (results from part B above) is plotted as filled circles. The solid lines are the results of the respective linear regression analyses. The vertical axis has the same scale as in part D below, i.e., it is marked in one linking number unit increments. (D) Plot of the temperature dependence of the linking number difference. The linking number difference (ΔL) between the polymerase-bound (determined from A; B) and bare (determined from C) DNA samples at each temperature is plotted for cNPR153 (λP_R promoter) (open circles, squares, and triangles, representing data from three separate determinations) and cLU857 (*lac*UV5 promoter) (filled circles and triangles, representing data from two separate determinations). The solid lines are fits to the data (see Materials and Methods and text).

single transition is 5.5 ± 0.5 °C for λP_R, which is markedly lower than that of *lac* UV5 and consistent with previous studies of λP_R (*10*, *57*). In addition, the difference in T_m values for the two promoters is consistent with the observation that different promoters exhibit distinct T_m values (*21*, *22*, *58*, *59*). Thus the results of the topological and chemical probe responses to temperature change specifically agree for two separate promoters and provide additional support for the proposal that the linking number change induced by open complex formation represents the opening of the transcription bubble.

The enthalpy (ΔH) value obtained from the fit to the *lac* UV5 data was 60 ± 9 kcal/mol; this is intermediate to the values obtained from kinetic [41 kcal/mol, (*60*)] and chemical probe [120 kcal/mol, (*22*)] studies. The value for λP_R was 76 ± 7 kcal/mol, which is larger than that obtained from kinetic studies [~30 kcal/mol, (*61*)]. However, different measurement methods have been found to give significantly different enthalpy values for bubble opening (*62*). The magnitude of the experimental errors in the values derived from topological analysis here indicates that the two promoters have comparable enthalpies of formation.

The Rate of Loss of the Linking Number Change after Temperature Downshift. The results in Figure 2 as well as those of chemical probe experiments (*21*, *22*) indicate that the predominate equilibrium forms of the *lac* UV5 promoter are an open complex above 30 °C and a closed complex below 12 °C. This information can be used to investigate a possible mechanism for the opening of the transcription bubble: it has been proposed that bubble opening involves using stress introduced into the DNA during formation of the open complex precursors (RPc, RPi) to drive bubble formation in RPo (*35*, *63*). The physical form of this stress could be duplex unwinding without denaturation (*64*, *65*)

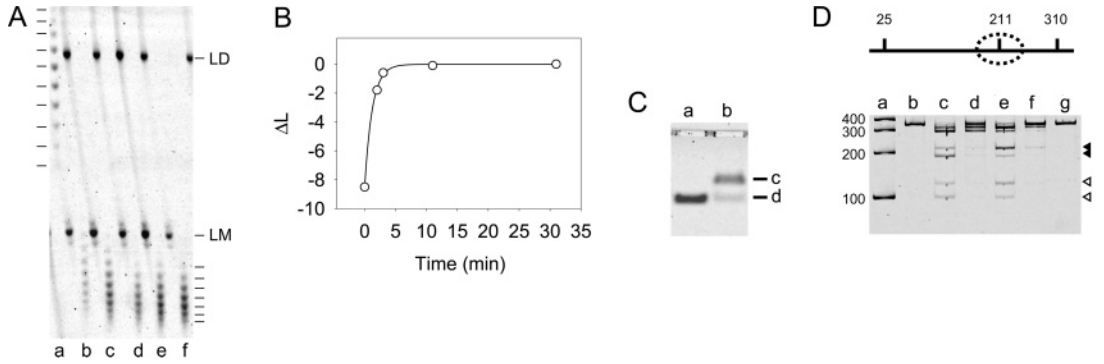

FIGURE 3: Kinetics of loss of linking number difference. Nicked cLU857 was incubated with RNA polymerase holoenzyme at 37 °C to form open complexes at the 8 *lac* UV5 promoters. Samples were then transferred to 12 °C and incubated for the indicated times, after which DNA ligase was added and the incubation was continued for 1 min to ligate the nicked circles. The purified DNA of each sample was then fractionated by two-dimensional electrophoresis in an agarose gel as in Figure 1. (A) An image of the ethidium-stained gel. The samples were (a) open complex sample ligated at 37 °C before temperature drop; (b) 1 min incubation at 12 °C; (c) 2 min incubation at 12 °C; (d) 10 min incubation at 12 °C; (e) 30 min incubation at 12 °C; (f) bare DNA ligated for 30 min at 12 °C. The mobilities of individual topoisomers of sample a are indicated at the upper left side of the gel, while those of samples b−f are indicated at the lower right of the gel. The mobilities of the linear monomer (**LM**) and linear dimer (**LD**) are indicated at the right of the gel. (B) A plot of the kinetics. Δ*L* is the difference between the linking number of the time point sample and that of the sample of bare DNA relaxed at 12 °C (i.e., the lane f sample). The value of the 0-time point (the lane a sample, ligated at 37 °C) has been corrected for the effect of the ligation temperature difference (37 °C vs 12 °C) on the total DNA of the circle. The time represents the incubation time plus the 1-minute ligation time at 12 °C. The solid line is the fit of a decay function to the data, which yielded a $t_{1/2} = 1.2$ min (C) Post-shift occupancy demonstrated by bandshift analysis. The 332 bp *Nci*I/*Psh*AI fragment (diagrammed at the top of Figure 3D) was incubated with RNA polymerase at 37 °C to form an open complex, after which the temperature was shifted to 12 °C and the sample incubated for a further 2 min. The sample was then immediately applied to an agarose gel equilibrated at 12 °C, followed by electrophoresis for 9 min (see Materials and Methods). The ethidium-stained gel is shown: (a) bare DNA; (b) polymerase-incubated sample. At the right are indicated the mobilities of the bandshifted polymerase-complex (c) and bare DNA (d). (D) Post-shift occupancy demonstrated by restriction digestion protection. The 332 bp *Nci*I/*Psh*AI fragment from pLU875 is diagrammed at the top (*Nci*I end on left). The *Hpa*II sites located at nt25, nt211, and nt310 from the *Nci*I end are indicated. The *lac* UV5 start site is at nt236 and transcription is to the right, while the extent of the open complex footprint (*20*, *89*, *90*) is indicated by the dashed-line oval. This fragment was incubated with RNA polymerase at 37 °C to form an open complex, after which half the sample was shifted to 12 °C and incubated for 2 min. *Hpa*II was then added to each sample and the incubation continued for an additional 2 min at the respective temperatures (see Materials and Methods). The extracted DNAs were then fractionated by electrophoresis in an acrylamide gel, which is shown at the bottom: (a) marker DNA; (b and g) untreated 332 bp fragment; (c) 37 °C bare DNA, *Hpa*II digested; (d) 37 °C sample plus polymerase, *Hpa*II digested; (e) 12 °C bare DNA sample, *Hpa*II digested; (f) 12 °C sample plus polymerase, *Hpa*II digested. The sizes of the markers in bp are indicated at the left. The bands marked with the arrowheads at the right side of the gel are all fragments that result from *Hpa*II digestion at nt211. The 186 and 211 bp bands (marked with filled arrowheads at right) in lanes c and e are fragments to the left of nt211 (see diagram at top) that result when that site is digested, while the 99 and 121 bp bands (marked with open arrowheads at right) are fragments to the right.

and/or left-handed superhelical DNA wrapping (*35*, *66*). This proposal derives from results of the analysis of the effect of supercoiling on the kinetics of *lac* UV5 open complex formation as well as wild type *lac* topological measurements: it was found that the negative linking change was present when the wild type complex should have been in the closed form (RPc and RPi), i.e., prior to open complex formation (*35*). To reinvestigate this possibility directly using our multicopy, homogeneous promoter system, we measured (Figure 3) the rate of loss of the open complex linking number change that occurs with a temperature shift of 37 °C (RPo) to 12 °C [RPi, although structural distinctions (*67*) have led to this being termed "RP_{LT}" as well (*15*)]. The equilibrium results in Figure 2 indicate that the maximal linking number change at 37 °C is virtually eliminated at 12 °C. Kinetic analysis and footprinting studies indicate that RPi persists [$t_{1/2} = 20$ min, (*60*)] well beyond the time of bubble collapse as measured by chemical probing [$t_{1/2} \cong 3$ min (*15*)]. Thus if the stress is retained as left-handed superhelical wrapping in RPi following bubble collapse (*35*), the loss of linking number change should take considerably longer than 3 min.

Figure 3 shows the rate of loss of the linking number change of the *lac* UV5 open complex when the temperature is shifted from 37 °C to 12 °C. Open complexes were formed by incubating polymerase with nicked cLU875 as in Figure 1, after which the sample was shifted to 12 °C. Samples were then removed at the indicated times and incubated with DNA ligase for 1 min, followed by fractionation of the extracted DNA by electrophoresis in an agarose gel. The image of the gel in Figure 3A shows that the topoisomer distribution of the sample that was ligated prior to the temperature drop (lane a) exhibits the low mobility indicative of the negative linking number change of the open complex (cf. Figure 1, lanes f−k). However, lowering the temperature to 12 °C causes a rapid loss of this linking number change: within 2 min (1 min incubation followed by 1 min ligation) of the temperature drop, most of the linking number deficit of the open complex has been lost. The quantification of these results in the graph in Figure 3B yields a $t_{1/2}$ of 1.2 min for the loss of the linking number deficit of the open complex. This is comparable to the rate observed in chemical probe experiments for bubble loss ($t_{1/2} \cong 3$ min) (*15*). In contrast, polymerase remains associated with the promoter for an hour or more following such a temperature downshift, as indicated by kinetic (*60*) and DNase I-footprinting (*68*) studies.

To confirm that this relatively slow rate of dissociation following a temperature downshift is indeed a property of our system as well, two methods that directly measure complex persistence were used. First, band shift analysis (Figure 3C) demonstrated that polymerase is still bound after

the linking number deficit has been lost. RNA polymerase was incubated at 37 °C to produce an open complex on a 332 bp fragment containing the *lac* UV5 promoter (fragment diagrammed at the top of Figure 3D). The temperature was then reduced to 12 °C and the incubation continued for an additional 2 min. The sample was immediately applied to an agarose gel equilibrated at 12 °C, and electrophoresis was performed for 9 min. Figure 3C, lane b, shows that after such treatment almost all the DNA is in a single bandshifted complex (marked c). This indicates that RNA polymerase remains bound well beyond 2 min at 12 °C.

While this bandshift result shows that polymerase remains bound well past 2 min, it does not show it is bound to the *lac* UV5 promoter, e.g., it could be bound to one of the DNA ends. To demonstrate that the polymerase is bound to the promoter, a second method was used: blockage to restriction enzyme digestion. Figure 3D (top) shows a diagram of a 332 bp fragment containing the *lac* UV5 promoter, with the locations of 3 *Hpa*II sites indicated. The size of RNA polymerase footprint (indicated by a dashed-line oval) from footprinting studies indicates that the *Hpa*II site at nt211 should be blocked when RNA polymerase is bound at the promoter. The gel in the lower part of Figure 3D shows the result of such an analysis of promoter occupancy. *Hpa*II digestion of bare DNA for 2 min at 37 °C (Figure 3D, lane c) produces a partial digest, with cleavage at nt211 indicated by fragments of 211 bp and 186 bp (originating from the left side of the nt211 site in the diagram and marked by solid arrowheads at the right of the gel) and fragments of 121 bp and 99 bp (originating from the right side of nt211 in the diagram and marked by open arrowheads at the right of the gel). When the 322 bp fragment is first incubated at 37 °C with RNA polymerase to form an open complex at the *lac* UV5 promoter (Figure 3D, lane d), these lower bands are absent in the *Hpa*II digest. The absence of these bands in the digest of the open complex demonstrates that blockage of *Hpa*II cleavage at nt 211 detects promoter occupancy. *Hpa*II digestion at 12 °C for 2 min on bare DNA (Figure 3D, lane e) also generates the lower bands characteristic of cleavage at nt211. Figure 3D, lane f, shows the results of incubation with polymerase at 37 °C to form an open complex, then dropping the temperature to 12 °C and incubating for 2 min, and finally digesting with *Hpa*II for an additional 2 min at 12 °C. The lack of lower bands at 211, 186, 121, and 99 bp demonstrates that cleavage at nt211 blocked. This means that polymerase is still bound to the *lac* UV5 promoter after a 2 min incubation at 12 °C and an additional 2 min *Hpa*II digestion at 12 °C, an incubation time period that results in the loss of virtually all of the linking number deficit. Thus the bandshift results (Figure 3C) and the restriction digestion protection results (Figure 3D) both demonstrate that RNA polymerase remains bound at the *lac* UV5 promoter well beyond the time at 12 °C required to eliminate the linking number deficit (Figure 3B). This indicates that the loss of linking number deficit is not simply due to dissociation of the RNA polymerase, but instead represents transition to a closed complex that is still bound to the DNA. Thus measurement of the rate of loss of the linking number change indicates that it derives entirely from bubble induction upon formation of the open complex and is not present in RPc or RPi as proposed (*35*).

Linking Number Change in Abortive Initiation Complexes. Additional support for a direct relationship between linking number change and the transcription bubble was obtained from an analysis of abortive transcription complexes. Recent single molecule studies (*69*−*71*) indicate that the transition from an open complex to an abortive complex involves an expansion of the transcription bubble. If there is a direct relationship between bubble size and linking number change, then the linking number change induced by formation of the abortive complex should be more negative than that of the open complex which was measured in Figures 1−3. To determine if this is in fact the case, open complexes were formed on *Nb.Bpu*10I-nicked cNPR149. Samples were then incubated with RNA oligoribonucleotides. In these conditions, the oligonucleotides were bound to the active center of RNA polymerase simulating the abortive products prior to their dissociation from the enzyme. The biochemical analysis done with the radioactively labeled RNA oligonucleotides confirmed their binding to RNA polymerase (data not shown). Samples were then treated with *E. coli* ligase to seal the nick, after which the extracted DNAs were fractionated by electrophoresis in an agarose gel.

The gel in the left part of Figure 4A shows that the topoisomer distribution of the open complex sample (lane a) has a center that is little different from that of the GUUGC (position −1) sample (lane b). However, the center of the UGCAU (+2) sample (lane c) is about +0.4 topoisomer spots higher in the gel, meaning that the formation of the +2 abortive complex here results in a linking number change of −0.4 relative to the open complex. The average (±SD) of 15 separate experiments was −0.62 ± 0.21 for this +2 complex. The centers of the GCAUG (+3) sample (lane d) and UGCAUG (+3) sample (lane e) distributions are essentially equal and higher still in the gel than that of the +2 complex. They exhibit a linking number change of about −1.6 relative to the open complex. The average for the GCAUG (+3) abortive complex was −1.62 ± 0.19 [average ± SD from the rotational variant analysis (*40*) that included 28 measurements of open complex and 30 measurements of the GCAUG (+3) complex].

Equivalent results were obtained when the +3 abortive complex was generated by transcription elongation, as shown in the experiment in the lower right of Figure 4A. As above, open complex was formed (lane f), followed by binding UGCAU to form the +2 complex (lane g), only at this point GTP was added (lanes h, i, j) to extend the UGCAU +2 complex to the UGCAUG +3 complex. As seen above, adding UGCAU to the open complex causes a change of about −0.6 relative to the open complex. Extension of this to UGCAUG +3 results in a change to −1.6 relative to the open complex, which is the same as seen above for direct binding of the complete UGCAUG.

The linking number change of −0.6 for the whole circle when the +2 complex is formed is $-0.06/\lambda P_R$, which corresponds to opening of about 0.6 bp of bubble, while the −1.6/circle change for the +3 complex corresponds to an opening of 1.6 bp (these numbers probably represent a lower estimate for the bubble extension during abortive initiation due to an intrinsic instability of the abortive complex, which tends to convert back to RPo by release of the RNA primers). Thus the direct relation between linking number change and the transcription bubble is further supported by this result.

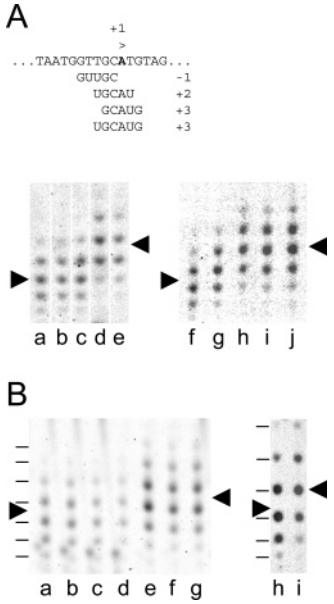

FIGURE 4: Topological effects of transcription complex bubble perturbation. (A) Analysis of abortive initiation complexes. At the top is shown the sequence surrounding the λP_R promoter start site, with the A at +1 in bold. Beneath are shown the oligoribonucleotides used in these experiments, with the sequence position of each 3′ end indicated at the right. For the gel on the left, *Nb.Bpu*10I-nicked cNPR147 was incubated with a saturating concentration of RNA polymerase to form an open complex (see Materials and Methods). Samples were then removed and further incubated with the indicated oligoribonucleotides, after which all samples incubated with *E. coli* DNA ligase to ligate the nick. The purified DNAs were then fractionated by one-dimensional electrophoresis in an agarose gel containing 0.02 μg/mL ethidium bromide. An image of the ethidium-stained gel is shown. The following oligoribonucleotides were included in the incubation with open complex (the number in parentheses indicates the position of the 3′ end): (a) no oligo (open complex); (b) GUUGC (−1); (c) UGCAU (+2); (d) GCAUG (+3); (e) UGCAUG (+3). The arrowhead on the left marks the center of the topoisomer distribution in lane a, while that to the right marks the center of the topoisomer distribution in lane d. The gel on the lower right represents a similar experiment in which open complex formed on cNPR149 (lane f) was incubated with UGCAU (lane g) to form a +2 abortive complex. This complex was then incubated with 0.75 μM GTP (lane h), 1.5 μM GTP (lane i), or 3.0 μM GTP (lane j) to extend the oligo by one nucleotide to generate a +3 abortive complex. (B**)** Magnesium effect on the linking number difference. Open complexes were formed on covalently closed, relaxed cNPR149 by incubation with RNA polymerase at 37 °C in the presence and absence of magnesium chloride, after which the complexes were relaxed with topoisomerase I. The extracted DNAs were then fractionated by two-dimensional electrophoresis in an agarose gel. The left panel shows the ethidium-stained image of a gel that contained 0.022 μg/mL ethidium bromide in the first dimension (top to bottom) and 0.1 μg/mL ethidium bromide in the short second dimension (left to right). The ratio of RNA polymerase to λP_R was (a) 6.8; (b) 10; (c) 13.5; (d) 16.9; (e) 6.8; (f) 10; (g) 16.9. Samples a−d were relaxed in the absence of magnesium chloride, while samples e−g were relaxed in the presence of 10 mM magnesium chloride. The dashes at the left of the gel indicate the mobilities of the topoisomers. The arrowhead at the left of the gel indicates the centers of the topoisomer distributions of samples a−d, while that at the right of the gel indicates the centers of samples e−g. The gel in the right panel contained 0.28 μg/mL chloroquine diphosphate in the first dimension and 0.1 μg/mL ethidium bromide in the short second dimension. The samples were bare DNA relaxed in the presence (h) and absence (i) of 10 mM magnesium chloride. The arrowhead at the left of the gel indicates the center of the topoisomer distribution of sample h, while that at the right indicates the center of sample i.

Moreover, it provides independent confirmation and an extension of the conclusions of the single molecule and FRET studies (*70*, *71*) about the mechanism of transcription initiation. This will be addressed further in the Discussion.

The Effect of Mg^{2+} on the Transcription Bubble Size. Kinetic analysis indicates that there are two open complexes that form at the λP_R promoter: RPo1 forms in the absence of Mg^{2+} and is a precursor to RPo2, which forms in the presence of Mg^{2+} and is the open complex that initiates transcription with addition of nucleotide triphosphates (*72*). A subsequent chemical probe study indicated a structural difference between the two complexes: the extent of $KMnO_4$ reactivity in the open complex formed at the λP_R promoter is at least 14 bp in the presence of Mg^{2+} but less than 12 bp in its absence (*10*). Similar results were obtained for other promoters (*11*, *12*). These results, combined with those from kinetic studies, were interpreted to mean that there is a ∼8−10 bp bubble in RPo1, and this is expanded to a ∼15 bp bubble that encompasses the transcription start site in the transition to the transcriptionally competent RPo2 (*10*). However, the interpretation of $KMnO_4$ reactivity in terms of bubble size is complicated by the possibility that neutralization of the negative charge of the DNA phosphate anions by Mg^{2+} may increase reactivity by increasing access of the negatively charged permanganate ion to the DNA. The result would be an increased extent of reactivity to permanganate in the presence of Mg^{2+} even in the absence of a change in bubble size (*17*, *24*−*26*).

DNA topological analysis is particularly well suited to the clarification of this ambiguity in the interpretation of chemical probe experiments. The ability of topology to measure the change in duplex rotation geometry that accompanies a change in bubble size can provide an independent evaluation of the permanganate results. Importantly, topological analysis of Mg^{2+} effects on DNA structure can be conveniently performed through the use of topoisomerase I, an enzyme that is active in the presence or absence of Mg^{2+} (*73*). For the type of circle used here containing 10 λP_R copies, the permanganate results (*10*) would predict that formation of open complexes in the presence of Mg^{2+} should produce a linking number change of about −14 to −15 [ΔL = (10 promoters) × (15 bp/bubble) × (−1 ΔL unit/10.5 bp) = −14.3], while those formed in the absence of Mg^{2+} should produce a linking number change of about −9 to −10 [ΔL = (10 promoters) × (10 bp/bubble) × (−1 ΔL unit/10.5 bp) = −9.5]. Such a difference is readily detected, since the precision of the measurement of ΔL is about ±0.1 linking number unit (*48*, *74*).

In the experiment of Figure 4B open complexes were formed in the presence and absence of Mg^{2+}, followed by incubation with topoisomerase I. The purified DNAs were then fractionated by electrophoresis in an agarose gel, and the image of the gel is shown in the left panel of Figure 4B. Lanes a−d show samples of open complexes formed in the presence of Mg^{2+} using increasing concentrations of polymerase. The centers of the distributions have essentially equivalent mobilities, indicating that the promoters are saturated at the polymerase concentrations used. The arrow at the left indicates this common center. Lanes e−g show a similar set of samples that were formed in the absence of Mg^{2+}. Again, the centers of the topoisomer distributions have essentially equivalent mobilities, indicating promoter satura-

tion, and the arrow on the right indicates this common center for these no-Mg^{2+} samples. The arrow on the left is slightly lower than that on the right, indicating that the linking number of the plus-Mg^{2+} sample is slightly higher than that of the no-Mg^{2+} sample. However, an equivalent change is seen in the bare DNA samples (right panel of Figure 4B), an effect that derives from Mg^{2+} winding up the duplex to produce an increase in the linking number (*73*, *75*). The linking number difference was calculated through the use of connector samples to relate the register of the two different gels (see Materials and Methods). The resultant ΔL for the no-Mg^{2+} sample was -9.4 ± 0.1 (average $\pm$ SD, 3 measurements), or $-0.94 \pm 0.01/\lambda P_R$. This corresponds to a bubble size of 9.9 ± 0.1 bp [$=(0.94) \times (10.5)$], a value that agrees with the value of 8−10 bp estimated from the permanganate measurement in the absence of Mg^{2+} (*10*). However, the ΔL measured for the $+Mg^{2+}$ sample was -9.5 ± 0.3 (average $\pm$ SD, 3 measurements), or $-0.95 \pm 0.03/\lambda P_R$. This corresponds to a bubble size of 10.0 ± 0.3 bp. This is virtually the same as the no-Mg^{2+} topological value but dramatically less than the permanganate probe $+Mg^{2+}$ value of 14−15 bp (*10*). Thus the topological results do not support the interpretation of the permanganate results that the bubble expands significantly upon addition of Mg^{2+}. This indicates that the more extensive permanganate reactivity in the presence of Mg^{2+} is likely due to an alternative effect such as neutralization of the negative charges of the DNA by Mg^{2+} (*17*, *24*−*26*) or local distortion of the duplex not associated with the DNA unwinding.

DISCUSSION

The current study employs a modified topological procedure to characterize the structure of the bubble in the open and abortive promoter complexes formed by *E. coli* RNA polymerase. These results extend the findings of earlier topological studies as well as complement and clarify the results of chemical probe characterizations of the bubble. The modifications employed in the current study include the use of a circle containing multiple copies of a single promoter. The amplification of signal that results from the multiple copies as well as the elimination of other promoters from the circle markedly improves the precision as well as the promoter specificity of the measurement relative to earlier topological studies (*31*−*35*, *38*, *39*). This allows a more detailed interpretation of the topological data in terms of open complex structure (see below).

The higher precision and specificity also mean that this modified topological method is more effective in complementing the chemical probe approach for the purpose of providing a more detailed picture of the transcription bubble in the open complex. As described above, strengths of the probe approach are the abilities to determine the location and approximate size of a bubble, but it suffers from uncertainties about the precise bubble size and the possibility that reactivity may result from distortions other than a bubble. A complementing strength of the topological method is its potential to quantify the change in duplex geometry resulting from the unwinding event, and that this measurement represents the total population of native, active complexes. However, chemical probe results can help to resolve the ambiguity in interpreting the structural origin of the linking number change: how much of the change is cause by a change in duplex winding (twist, e.g., bubble formation) and how much is due to a change in the path of the DNA duplex (writhe, e.g., superhelical wrapping of DNA on the surface of polymerase).

For the open complex, we propose that essentially all of the linking number change derives from duplex unwinding of bubble formation with minimal contribution from superhelical wrapping. This is based on the following reasons. First, the linking number changes measured for the *lac* UV5 and λP_R promoters both agree well with the semiquantitative estimates of bubble size from the respective probe experiments. Thus there is no substantial discrepancy that could be assigned to superhelical wrapping. Second, the open complex linking number change is lost in a single abrupt transition as the temperature is reduced (Figure 2), and this corresponds to the loss of chemical probe reactivity for *lac* UV5 (*21*, *22*): both methods show a T_m of about 20 °C. Third, the rate of loss of open complex linking number change upon temperature reduction to below the T_m (Figure 3A,B) matches the rate of loss of chemical probe reactivity at *lac* UV5 (*15*), even though the polymerase remains associated (as RPc or RPi) with the promoter for a considerably longer time at low temperature [Figure 3C,D; (*60*, *68*)]. The loss of linking number change is complete, indicating there is no remaining superhelical wrapping in the complex following bubble collapse, even though footprinting results indicate that extensive polymerase−promoter contacts (wrapping) remain in RPc (*68*). Fourth, incubating the λP_R open complex with oligoribonucleotides that extend to +2 and +3, as well as extending the +2 oligonucleotide to +3, results in a linking number change that is progressively more negative than that of the open complex. This indicates that the bubble has expanded at the downstream end to accommodate the RNA hybrid, providing further evidence that the linking number change quantifies bubble size. In addition, as described below, the indicated increases in bubble size are consistent with the result of independent studies employing FRET and single molecule methodologies (*69*−*71*).

As described in the introduction, a previous topological study by Amouyal and Buc (*35*) measured a linking number change of −1.7 for both the *lac* wild type and *lac* UV5 promoters. This is ∼−0.7 in excess of the ∼−1.0 predicted by the probe experiments for the bubble, and they proposed that this apparent excess represents a left-handed superhelical wrap of about 0.7 turn on the polymerase surface. This is widely cited as the first evidence for superhelical wrapping in the open complex [e.g., (*37*, *76*−*78*)]. In addition, evidence was presented (*35*) for the existence of this wrapping in the closed precursor (RPi, see introduction) to the open complex (RPo). These findings served as the basis of a model for the mechanism by which the duplex is melted in the formation of the open complex: the bending energy present in the wrapping in RPi serves to drive the bubble opening in the transition to RPo [(*35*, *63*), see also (*78*)].

Two of the main findings in the current study eliminate much of the basis for this model. First, the improved precision of the multicopy, single promoter system used here generates a value of −1.17/*lac* UV5 promoter. This is approximately equal to that expected from the results of the chemical probe experiments (*21*, *22*), and thus eliminates the basis for predicting superhelical DNA wrapping in the open complex. We propose that their larger value of −1.7

(*35*) is likely due to limited precision deriving from the plasmids used: the measurement was of a difference of differences between two plasmids that differed in the presence of a single *lac* UV5 promoter, with the vector promoters in each plasmid contributing the predominant portion of the overall linking number change (i.e., measurement of a small difference between two large numbers). These design problems were addressed with the multicopy, single promoter constructs analyzed here. For reference, a change of −1.7/*lac* UV5 (*35*) in the 8-copy cLU875 construct here would result in $\Delta L = -13.6$, a linking number change readily distinguished from the $\Delta L = -9.38 \pm 0.02$ that was measured (Figure 1). Second, the kinetic analysis in Figure 3A,B demonstrates that the open complex ΔL is virtually eliminated within 5 min of the temperature drop, while RPc/RPi persists well beyond that [Figure 3C,D; (*60*, *68*)]. This indicates that RPc/RPi does not contain superhelical DNA wrapping on the polymerase, eliminating a left-handed wrap as the source of energy for unwinding the duplex in the transition to RPo. In conclusion, the results in Figures 1 and 3 make unlikely a mechanism in which left-handed superhelical wrapping drives open complex bubble formation (*35*, *63*).

One difference between our study and that of Amouyal and Buc is that our construct contains *lac* UV5 upstream sequence to −59 while that of Amouyal and Buc extends to −140. Singlet oxygen footprinting indicates an interaction at −90 (*79*), raising the possibility that the DNA could be pulled around to contact a site upstream of −59 to cause a wrap. However, atomic force microscopy (*80*) of a −146 *lac* UV5 construct does not observe contour length shortening that is consistent with extensive wrapping. They propose that upstream contacts indicated by cross-linking and footprinting results may be transient and not representative of the total population of complexes at equilibrium. We feel that these findings as well as those indicating that upstream interactions are non-sequence-dependent (*23*) argue that the lower magnitude of ΔL obtained here is not due to the difference in far upstream sequence compared to Amouyal and Buc but rather to a difference in precision due to experimental design.

The finding here that there is not the excess ∼−0.5 linking number change that can be assigned to left-handed wrapping does not rule out the possibility of wrapping on, or perhaps more precisely stated, extensive contact with, the surface of the polymerase. Biochemical analysis of interaction of RNA polymerase the DNA in the open promoter complex using DNase I footprinting, chemical probe footprinting, and protein−DNA cross-linking strongly suggest that promoter DNA extensively contacts the surface of the enzyme [reviewed in (*37*)]. Microscopy studies (*80*−*82*) also suggest that open complex DNA may be wrapped on the surface, although questions about the effects of adsorption of the complexes to a surface complicates interpretation of these studies (*83*). However, these methods do not specify the path of the DNA in contact with the polymerase, and in particular, none of these methods distinguish between wrapping that will or will not cause a change in linking number (writhe). Only wrapping that leads to an excess of DNA duplex crossings of one hand over another (chiral wrapping, such as in a superhelix) will result in a linking number change (*27*). For example, if promoter DNA is bent in a plane when it binds polymerase, no linking number change will result. Similarly, bending that results in an equal number of right-handed and left-handed crossings will result in no change. Thus the substantial contacts with the surface of the polymerase that are indicated by the various studies described above will only result in a linking number change if that wrapping is chiral [e.g., in the form of a superhelix; see (*40*)].

A recent footprinting study (*84*) proposes that an intermediate initiation complex (I_1) at λP_R is wrapped extensively in a right-handed superhelix, but that a significant amount of the footprint is lost upon conversion to open complex. If the remaining footprint in the open complex represents a small amount of remaining right-handed superhelix, then it would perhaps be apparent in the topology results here. Deducing this depends on how the chemical probe results are interpreted. Thus 8 to 15 bp of DNA at the λP_R start site are reactive with permanganate (*10*), although, as discussed above, there are numerous caveats concerning quantitative interpretation of this reactivity in terms of bubble size. If the upper end of the range of the permanganate results (∼14 bp) does in fact represent the actual bubble size, then $\Delta L = \Delta T = -14/10.5 = -1.3$, a value that is more negative than the $\Delta L = -0.983$ measured here for the λP_R promoter. An implication of this difference is that the open complex could contain approximately 0.3 turn of right-handed superhelical wrap (thus $\Delta W = +0.3$, so $\Delta L = \Delta T + \Delta W = -1.3 + 0.3 = \sim -0.983$). Of course this prediction depends critically on the reliability of the interpretation of the permanganate data in terms of unwound duplex, e.g., if the 10.5 bp of reactivity represents the true size of unwinding, then $\Delta T = -1.0$ and no superhelical (chiral) wrapping is implied.

While the linking number change is not as negative as −1.7 for either promoter, it is distinctly more negative for the *lac* UV5 promoter ($\Delta L = -1.17 \pm 0.01$, Figure 1) than for the λP_R promoter [$\Delta L = -0.94 \pm 0.01$ from Figure 1; -0.95 ± 0.03 from Figure 4; -0.983 ± 0.006 from (*40*)]. It is possible that the additional −0.2 that *lac* UV5 exhibits relative to λP_R reflects the difference in spacing between the −35 and −10 regions of the two promoters. The spacing is a consensus 17 bp for the λP_R promoter, but it is 18 bp for the *lac* UV5 promoter (*86*), i.e., one nucleotide longer than the consensus length. Thus binding the −35 and −10 regions to their respective sites on RNA polymerase could require the *lac* UV5 promoter to be unwound by the equivalent of about one additional base pair compared to the λP_R promoter (*87*). This difference would translate to about −0.1 in additional linking number change for *lac* UV5. This is in reasonable agreement with the value of −0.2 measured, especially when one considers that the sequence difference in the −10 to −35 regions of the two promoters means that the overall screws will differ to some degree. A similar difference was also observed in linking number measurements of open complexes on two spacer length variants of the TAC promoter (*38*), a study that supports the proposal that spacer length has an effect on promoter strength (*87*). Overall, the findings here support an alteration in the DNA structure (*87*) to accommodate the difference in promoter spacing. They do not support the alternative proposal that the structure of the polymerase is altered to accommodate the spacing difference (*88*).

In addition to resolving issues concerning the role of superhelical wrapping of DNA in the open complex forma-

tion, the results of this high precision topological measurement system also clarify the effect of Mg^{2+} on bubble size in the open complex (Figure 4B). The extensive use of chemical probe analysis to detect and characterize the transcription bubble underscores the importance of establishing the degree to which chemical probe reactivity describes bubble structure. As discussed above, numerous features of the probe reaction raise significant uncertainties about interpretation in structural terms, but a parallel topological analysis can resolve many of these. Thus the topological measurements in Figure 4B indicate that the bubble size is essentially the same in the presence and absence of Mg^{2+}. This indicates that the expanded permanganate reactivity at the promoter in the presence of Mg^{2+} (*10*, *11*) is likely caused by the ability of Mg^{2+} to mask the negative charge of promoter DNA phosphates, and is not an indication of a larger transcription bubble. The topological results reported here provide significant independent support for the concerns raised about the ability of chemical probe experiments to unambiguously characterize the transcription bubble (*17*, *24*−*26*), thereby permitting a more informed interpretation of future probe results. Moreover, these results indicate that the RPo1 and RPo2 transcription initiation intermediates that have been identified by kinetic analysis are not structurally distinguishable by bubble size as proposed (*10*).

Finally, the results here for abortive complexes independently confirm and extend the conclusions of recent studies concerning the mechanism of transcription initiation. Results from FRET (*70*) and single molecule (*71*) studies indicate the DNA is pulled into the polymerase when the first nucleotides of RNA are synthesized during abortive initiation. The authors term this process "DNA scrunching". The result of this is an increase in the size of the transcription bubble that reflects the extent of RNA synthesis. Revyakin et al. (*71*) conclude that the bubble expands in proportion to bases synthesized once 2 ± 1 base are made. Thus they propose that increases in unwinding equal to $N - 2$, with N equal to the length of RNA in nucleotides. Our findings here support and refine this proposal through an independent methodology, DNA topology. Thus the +2 complex exhibits $\Delta L = -0.062 \pm 0.021$ relative to the open complex, which corresponds to and additional 0.65 ± 0.22 bp unwound. The +3 complex exhibits $\Delta L = -0.160 \pm 0.019$ relative to open complex, corresponding to 1.68 ± 0.20 bp unwound. Thus the bp unwound equals the bp synthesized, independently confirming the results of Revyakin et al. (*71*), but not until +1.4 s reached. Accordingly, we would refine the "$N - 2$" rule of Revyakin et al. (*71*) to $N - 1.4$. Importantly, all three studies provide consistent support for a model in which polymerase draws the DNA into itself in the initial stages of transcription, with the result that the transcription bubble increases in size.

ACKNOWLEDGMENT

We would like to thank Olga Shabalin for excellent technical assistance and Dr. Lucyna Lubkowska for providing essential materials. The contents of this publication do not necessarily reveal the views or policies of the Department of Health and Human Services, nor does mention of trade names, commercial product, or organizations imply endorsement by the U.S. Government.

REFERENCES

1. deHaseth, P. L., Zupancic, M. L., and Record, M. T., Jr. (1998) RNA polymerase-promoter interactions: the comings and goings of RNA polymerase, *J. Bacteriol. 180*, 3019−3025.
2. Record, M. T. Jr., Reznikoff, W. S., Craig, M. L., McQuade, K. L., and Schlax, P. J. (1996) *Escherichia coli* RNA polymerase ($E\sigma^{70}$), promoters, and the kinetics of the steps of transcirption initiation, in *Escherichia coli and Salmonella typhimurium: Cellular and Molecular Biology* (Neidhardt, F. C., Ed.) pp 792−821, ASM Press, Washington, DC.
3. Boeger, H., Bushnell, D. A., Davis, R., Griesenbeck, J., Lorch, Y., Strattan, J. S., Westover, K. D., and Kornberg, R. D. (2005) Structural basis of eukaryotic gene transcription, *FEBS Lett. 579*, 899−903.
4. Vassylyev, D. G., Vassylyeva, M. N., Zhang, J., Palangat, M., Artsimovitch, I., and Landick, R. (2007) Structural basis for substrate loading in bacterial RNA polymerase, *Nature*, advanced online publication. doi:10.1038/nature05931.
5. Vassylyev, D. G., Vassylyeva, M. N., Perederina, A., Tahirov, T. H., and Artsimovitch, I. (2007) Structural basis for transcription elongation by bacterial RNA polymerase, *Nature*, advanced online publication. doi:10.1038/nature05932.
6. Duval-Valentin, G., and Ehrlich, R. (1987) Dynamic and structural characterisation of multiple steps during complex formation between E. coli RNA polymerase and the tetR promoter from pSC101, *Nucleic Acids Res. 15*, 575−594.
7. Siebenlist, U. (1979) RNA polymerase unwinds an 11-base pair segment of a phage T7 promoter, *Nature 279*, 651−652.
8. Siebenlist, U., Simpson, R. B., and Gilbert, W. (1980) E. coli RNA polymerase interacts homologously with two different promoters, *Cell 20*, 269−281.
9. Sasse-Dwight, S., and Gralla, J. D. (1989) KMnO4 as a probe for lac promoter DNA melting and mechanism in vivo, *J. Biol. Chem. 264*, 8074−8081.
10. Suh, W. C., Ross, W., and Record, M. T. Jr. (1993) Two open complexes and a requirement for Mg2+ to open the lambda PR transcription start site, *Science 259*, 358−361.
11. Zaychikov, E., Denissova, L., Meier, T., Gotte, M., and Heumann, H. (1997) Influence of Mg2+ and temperature on formation of the transcription bubble, *J. Biol. Chem. 272*, 2259−2267.
12. Chen, Y. F., and Helmann, J. D. (1997) DNA-melting at the Bacillus subtilis flagellin promoter nucleates near -10 and expands unidirectionally, *J. Mol. Biol. 267*, 47−59.
13. Buckle, M., and Buc, H. (1989) Fine mapping of DNA single-stranded regions using base-specific chemical probes: study of an open complex formed between RNA polymerase and the lac UV5 promoter, *Biochemistry 28*, 4388−4396.
14. Severinov, K., and Darst, S. A. (1997) A mutant RNA polymerase that forms unusual open promoter complexes, *Proc. Natl. Acad. Sci. U.S.A. 94*, 13481−13486.
15. Brodolin, K., and Buckle, M. (2001) Differential melting of the transcription start site associated with changes in RNA polymerase-promoter contacts in initiating transcription complexes, *J. Mol. Biol. 307*, 25−30.
16. Lutter, L. C., and Kurland, C. G. (1973) Reconstitution of active ribosomes with crosslinked proteins, *Nat. New Biol. 243*, 15−17.
17. Lozinski, T., and Wierzchowski, K. L. (2003) Inactivation and destruction by KMnO4 of Escherichia coli RNA polymerase open transcription complex: recommendations for footprinting experiments, *Anal. Biochem. 320*, 239−251.
18. Kashlev, M., and Komissarova, N. (2002) Transcription termination: primary intermediates and secondary adducts, *J. Biol. Chem. 277*, 14501−14508.
19. Johnsrud, L. (1978) Contacts between Escherichia coli RNA polymerase and a lac operon promoter, *Proc. Natl. Acad. Sci. U.S.A. 75*, 5314−5318.
20. Carpousis, A. J., and Gralla, J. D. (1985) Interaction of RNA polymerase with lacUV5 promoter DNA during mRNA initiation and elongation. footprinting, methylation, and rifampicin-sensitivity changes accompanying transcription initiation, *J. Mol. Biol. 183*, 165−177.
21. Kirkegaard, K., Buc, H., Spassky, A., and Wang, J. C. (1983) Mapping of single-stranded regions in duplex DNA at the sequence level: single-strand-specific cytosine methylation in RNA polymerase-promoter complexes, *Proc. Natl. Acad. Sci. U.S.A. 80*, 2544−2548.
22. Spassky, A., Kirkegaard, K., and Buc, H. (1985) Changes in the DNA structure of the lac UV5 promoter during formation of an

open complex with Escherichia coli RNA polymerase, *Biochemistry 24*, 2723−2731.
23. Ross, W., and Gourse, R. L. (2005) Sequence-independent upstream DNA-alphaCTD interactions strongly stimulate Escherichia coli RNA polymerase-lacUV5 promoter association, *Proc. Natl. Acad. Sci. U.S.A. 102*, 291−296.
24. Craig, M. L., Suh, W. C., and Record, M. T. Jr. (1995) HO. and DNase I probing of E sigma 70 RNA polymerase−lambda PR promoter open complexes: Mg2+ binding and its structural consequences at the transcription start site, *Biochemistry 34*, 15624−15632.
25. Lozinski, T., and Wierzchowski, K. L. (2001) Mg^{2+} ions do not induce expansion of the melted DNA region in the open complex formed by Escherichia coli RNA polymerase at a cognate synthetic Pa promoter. a quantitative $KMnO_4$ footprinting study, *Acta Biochim. Pol. 48*, 495−510.
26. Lozinski, T., and Wierzchowski, K. L. (2005) Mg2+-modulated KMnO4 reactivity of thymines in the open transcription complex reflects variation in the negative electrostatic potential along the separated DNA strands. Footprinting of Escherichia coli RNA polymerase complex at the lambdaP(R) promoter revisited, *FEBS J. 272*, 2838−2853.
27. Crick, F. H. (1976) Linking numbers and nucleosomes, *Proc. Natl. Acad. Sci. U.S.A. 73*, 2639−2643.
28. Bauer, W. R., Crick, F. H., and White, J. H. (1980) Supercoiled DNA, *Sci. Am. 243*, 100−113.
29. Calladine, C. R., and Drew, H. R. (1992) DNA Supercoiling, in *Understanding DNA*, pp 114−133, Academic Press, London.
30. Sinden, R. R. (1994) *DNA Structure and Function*, Academic Press, San Diego, New York.
31. Saucier, J., and Wang, J. C. (1972) Angular alteration of the DNA helix by E. coli RNA polymerase, *Nat. New Biol. 239*, 167−170.
32. Wang, J. C., Jacobsen, J. H., and Saucier, J. M. (1977) Physiochemical studies on interactions between DNA and RNA polymerase. Unwinding of the DNA helix by Escherichia coli RNA polymerase, *Nucleic Acids Res. 4*, 1225−1241.
33. Gamper, H. B., and Hearst, J. E. (1982) A topological model for transcription based on unwinding angle analysis of E. coli RNA polymerase binary, initiation and ternary complexes, *Cell 29*, 81−90.
34. Gamper, H. B., and Hearst, J. E. (1983) Size of the unwound region of DNA in Escherichia coli RNA polymerase and calf thymus RNA polymerase II ternary complexes, *Cold Spring Harbor Symp. Quant. Biol. 47*, 455−461.
35. Amouyal, M., and Buc, H. (1987) Topological unwinding of strong and weak promoters by RNA polymerase. A comparison between the lac wild-type and the UV5 sites of Escherichia coli, *J. Mol. Biol. 195*, 795−808.
36. Finch, J. T., Lutter, L. C., Rhodes, D., Brown, R. S., Rushton, B., Levitt, M., and Klug, A. (1977) Structure of nucleosome core particles of chromatin, *Nature 269*, 29−36.
37. Coulombe, B., and Burton, Z. F. (1999) DNA bending and wrapping around RNA polymerase: a "revolutionary" model describing transcriptional mechanisms, *Microbiol. Mol. Biol. Rev.* (Washington, DC) *63*, 457−478.
38. Su, T. T., and McClure, W. R. (1994) Selective binding of Escherichia coli RNA polymerase to topoisomers of minicircles carrying the TAC16 and TAC17 promoters, *J. Biol. Chem. 269*, 13511−13521.
39. Bertrand-Burggraf, E., Schnarr, M., Lefevre, J. F., and Daune, M. (1984) Effect of superhelicity on the transcription from the tet promoter of pBR322. abortive initiation and unwinding experiments, *Nucleic Acids Res. 12*, 7741−7752.
40. Tchernaenko, V., Radlinska, M., Lubkowska, L., Halvorson, H. R., Kashlev, M., and Lutter, L. C. (2008) DNA bending in transcription initiation, *Biochemistry*, *47*, 1885−1895.
41. Ross, W., Thompson, J. F., Newlands, J. T., and Gourse, R. L. (1990) E.coli Fis protein activates ribosomal RNA transcription in vitro and in vivo, *EMBO J. 9*, 3733−3742.
42. Radlinska, M., Drabik, C. E., Tong, W. S., and Lutter, L. C. (2001) Generating tandem repeats by cloning with double initiator fragments, *BioTechniques 31*, 340−347.
43. Komissarova, N., and Kashlev, M. (1997) Transcriptional arrest: Escherichia coli RNA polymerase translocates backward, leaving the 3′ end of the RNA intact and extruded, *Proc. Natl. Acad. Sci. U.S.A. 94*, 1755−1760.
44. Lutter, L. C., Drabik, C. E., and Halvorson, H. R. (2000) Use of topology to measure protein-induced DNA bend and unwinding angles, in *Protein−DNA Interactions: A Practical Approach* (Travers, A. A., and Buckle, M., Eds.) pp 47−64, Oxford University Press, Oxford.
45. Lutter, L. C. (1989) Thermal unwinding of simian virus 40 transcription complex DNA, *Proc. Natl. Acad. Sci. U.S.A. 86*, 8712−8716.
46. Lutter, L. C., Judis, L., and Paretti, R. F. (1992) The effects of histone acetylation on chromatin topology in vivo, *Mol. Cell. Biol. 12*, 5004−5014.
47. Drabik, C. E., Nicita, C. A., and Lutter, L. C. (1997) Measurement of the linking number change in transcribing chromatin, *J. Mol. Biol. 267*, 794−806.
48. Tchernaenko, V., Radlinska, M., Drabik, C. E., Bujnicki, J. M., Halvorson, H. R., and Lutter, L. C. (2003) Topological measurement of the A-tract bend angle: comparison of bent and straightened states, *J. Mol. Biol. 326*, 737−749.
49. Cozzarelli, N. R., Boles, T. C., and White, J. H. (1990) Primer on the topology and geometry of DNA supercoiling, in *DNA Topology and its Biological Effects* (Cozzarelli, N. R., and Wang, J. C., Eds.) pp 139−184, Cold Spring Harbor Laboratory Press, Cold Spring Harbor.
50. Eadara, J. K., Hadlock, K. G., and Lutter, L. C. (1996) Chromatin structure and factor site occupancies in an in vivo-assembled transcription elongation complex, *Nucleic Acids Res. 24*, 3887−3895.
51. Hadlock, K. G., and Lutter, L. C. (1990) T-antigen is not bound to the replication origin of the simian virus 40 late transcription complex, *J. Mol. Biol. 215*, 53−65.
52. Kulaeva, O. I., and Lutter, L. C. (2001) TATA Box Occupancy in the SV40 Transcription Elongation Complex, *Virology 285*, 119−127.
53. Lutter, L. C., Halvorson, H. R., and Calladine, C. R. (1996) Topological measurement of protein-induced DNA bend angles, *J. Mol. Biol. 261*, 620−633.
54. Pindolia, K., and Lutter, L. C. (2005) Purification and characterization of the simian virus 40 transcription complex, *J. Mol. Biol. 349*, 922−932.
55. Depew, D. E., and Wang, J. C. (1975) Conformational fluctuations of DNA helix, *Proc. Natl. Acad. Sci. U.S.A. 72*, 4275−4279.
56. Pulleyblank, D. E., Shure, M., Tang, D., Vinograd, J., and Vosberg, H. P. (1975) Action of nicking-closing enzyme on supercoiled and nonsupercoiled closed circular DNA: formation of a Boltzmann distribution of topological isomers, *Proc. Natl. Acad. Sci. U.S.A. 72*, 4280−4284.
57. Craig, M. L., Tsodikov, O. V., McQuade, K. L., Schlax, P. E., Jr., Capp, M. W., Saecker, R. M., and Record, M. T., Jr. (1998) DNA footprints of the two kinetically significant intermediates in formation of an RNA polymerase-promoter open complex: evidence that interactions with start site and downstream DNA induce sequential conformational changes in polymerase and DNA, *J. Mol. Biol. 283*, 741−756.
58. Grimes, E., Busby, S., and Minchin, S. (1991) Different thermal energy requirement for open complex formation by Escherichia coli RNA polymerase at two related promoters, *Nucleic Acids Res. 19*, 6113−6118.
59. Duval-Valentin, G., and Ehrlich, R. (1986) Interaction between E. coli RNA polymerase and the tetR promoter from pSC101: homologies and differences with other E. coli promoter systems from close contact point studies, *Nucleic Acids Res. 14*, 1967−1983.
60. Buc, H., and McClure, W. R. (1985) Kinetics of open complex formation between Escherichia coli RNA polymerase and the lac UV5 promoter. evidence for a sequential mechanism involving three steps, *Biochemistry 24*, 2712−2723.
61. Roe, J. H., and Record, M. T., Jr. (1985) Regulation of the kinetics of the interaction of Escherichia coli RNA polymerase with the lambda PR promoter by salt concentration, *Biochemistry 24*, 4721−4726.
62. Leirmo, S., and Record, M. T., Jr. (1990) Structural, Thermodynamic and Kinetic Studies of the Interaction of $E\sigma^{70}$ RNA Polymerase with Promoter DNA, in *Nucleic Acids and Molecular Biology* (Eckstein, F., and Lilley, D. M. J., Eds.) Vol. 4, pp 123−151, Springer-Verlag, Berlin.
63. Buc, H. (1986) Mechanism of activation of transcription by the complex formed between cyclic AMP and its receptor in Escherichia coli, *Biochem. Soc. Trans. 14*, 196−199.
64. Saecker, R. M., Tsodikov, O. V., McQuade, K. L., Schlax, P. E., Jr., Capp, M. W., and Record, M. T. Jr. (2002) Kinetic studies and structural models of the association of E. coli sigma(70) RNA polymerase with the lambdaP(R) promoter: large scale confor-

mational changes in forming the kinetically significant intermediates, *J. Mol. Biol. 319*, 649−671.
65. Kontur, W. S., Saecker, R. M., Davis, C. A., Capp, M. W., and Record, M. T., Jr. (2006) Solute probes of conformational changes in open complex (RPo) formation by Escherichia coli RNA polymerase at the lambdaPR promoter: evidence for unmasking of the active site in the isomerization step and for large-scale coupled folding in the subsequent conversion to RPo, *Biochemistry 45*, 2161−2177.
66. Buc, H., and Amouyal, M. (1992) Superhelix Density as an Intensive Thermodynamic Variable, in *Nucleic Acids and Molecular Biology* (Eckstein, F., and Lilley, D. M. J., Eds.) pp 23−54, Springer-Verlag, Berlin.
67. Buckle, M., Pemberton, I. K., Jacquet, M. A., and Buc, H. (1999) The kinetics of sigma subunit directed promoter recognition by E. coli RNA polymerase, *J. Mol. Biol. 285*, 955−964.
68. Kovacic, R. T. (1987) The 0° C closed complexes between Escherichia coli RNA polymerase and two promoters, T7−A3 and lac UV5, *J. Biol. Chem. 262*, 13654−13661.
69. Roberts, J. W. (2006) Biochemistry. RNA polymerase, a scrunching machine, *Science 314*, 1097−1098.
70. Kapanidis, A. N., Margeat, E., Ho, S. O., Kortkhonjia, E., Weiss, S., and Ebright, R. H. (2006) Initial transcription by RNA polymerase proceeds through a DNA-scrunching mechanism, *Science 314*, 1144−1147.
71. Revyakin, A., Liu, C., Ebright, R. H., and Strick, T. R. (2006) Abortive initiation and productive initiation by RNA polymerase involve DNA scrunching, *Science 314*, 1139−1143.
72. Suh, W. C., Leirmo, S., and Record, M. T., Jr. (1992) Roles of Mg2+ in the mechanism of formation and dissociation of open complexes between Escherichia coli RNA polymerase and the lambda PR promoter: kinetic evidence for a second open complex requiring Mg2+, *Biochemistry 31*, 7815−7825.
73. Tchernaenko, V., Halvorson, H. R., and Lutter, L. C. (2004) Topological measurement of an A-tract bend angle: effect of magnesium, *J. Mol. Biol. 341*, 55−63.
74. Lutter, L. C., Tchernaenko, V., Radlinska, M., Drabik, C. E., Bujnicki, J. M., and Halvorson, H. R. (2002) Measurement of DNA bend angles using DNA topology, in *New Approaches to Structural Mechanics, Shells and Biological Structures* (Drew, H. R., and Pellegrino, S. Eds.) pp 475−484, Kluwer, Dordrecht.
75. Anderson, P., and Bauer, W. (1978) Supercoiling in closed circular DNA: dependence upon ion type and concentration, *Biochemistry 17*, 594−601.
76. Shin, M., Song, M., Rhee, J. H., Hong, Y., Kim, Y. J., Seok, Y. J., Ha, K. S., Jung, S. H., and Choy, H. E. (2005) DNA looping-mediated repression by histone-like protein H-NS: specific requirement of Esigma70 as a cofactor for looping, *Genes Dev. 19*, 2388−2398.
77. Maurer, S., Fritz, J., Muskhelishvili, G., and Travers, A. (2006) RNA polymerase and an activator form discrete subcomplexes in a transcription initiation complex, *EMBO J. 25*, 3784−3790.
78. Bates, A. D., and Maxwell, A. (2005) *DNA Topology*, IRL Press at Oxford University Press, Oxford.
79. Buckle, M., Buc, H., and Travers, A. A. (1992) DNA deformation in nucleoprotein complexes between RNA polymerase, cAMP receptor protein and the lac UV5 promoter probed by singlet oxygen, *EMBO J. 11*, 2619−2625.
80. Cellai, S., Mangiarotti, L., Vannini, N., Naryshkin, N., Kortkhonjia, E., Ebright, R. H., and Rivetti, C. (2007) Upstream promoter sequences and alphaCTD mediate stable DNA wrapping within the RNA polymerase-promoter open complex, *EMBO Rep. 8*, 271−278.
81. Rivetti, C., Guthold, M., and Bustamante, C. (1999) Wrapping of DNA around the E. coli RNA polymerase open promoter complex, *EMBO J. 18*, 4464−4475.
82. Rees, W. A., Keller, R. W., Vesenka, J. P., Yang, G., and Bustamante, C. (1993) Evidence of DNA bending in transcription complexes imaged by scanning force microscopy, *Science 260*, 1646−1649.
83. Meyer-Almes, F. J., Heumann, H., and Porschke, D. (1994) The structure of the RNA polymerase-promoter complex. DNA-bending-angle by quantitative electrooptics, *J. Mol. Biol. 236*, 1−6.
84. Davis, C. A., Bingman, C. A., Landick, R., Record, M. T. Jr., and Saecker, R. M. (2007) Real-time footprinting of DNA in the first kinetically significant intermediate in open complex formation by Escherichia coli RNA polymerase, *Proc. Natl. Acad. Sci. U.S.A. 104*, 7833−7838.
85. This reference was deleted on revision.
86. Murakami, K. S., Masuda, S., Campbell, E. A., Muzzin, O., and Darst, S. A. (2002) Structural basis of transcription initiation: an RNA polymerase holoenzyme-DNA complex, *Science 296*, 1285−1290.
87. Stefano, J. E., and Gralla, J. D. (1982) Spacer mutations in the lac ps promoter, *Proc. Natl. Acad. Sci. U.S.A. 79*, 1069−1072.
88. Murakami, K. S., and Darst, S. A. (2003) Bacterial RNA polymerases: the wholo story, *Curr. Opin. Struct. Biol. 13*, 31−39.
89. Schmitz, A., and Galas, D. J. (1979) The interaction of RNA polymerase and lac repressor with the lac control region, *Nucleic Acids Res. 6*, 111−137.
90. Straney, D. C., and Crothers, D. M. (1985) Intermediates in transcription initiation from the E. coli lac UV5 promoter, *Cell 43*, 449−459.

BI701289G